



Numerical Analysis of Mixed Convection in a Ventilated Closed Cavity

Lyes NASSERI¹, Zouhira HIRECHE¹, Djamel Eddine AMEZIANI¹

¹FGMGP/USTHB, B.P.32, El Allia BabEzzouar 16111, Algiers, Algeria

lnasseri@usthb.dz, zouhireche@yahoo.fr, deameziani@usthb.dz

Abstract.

The convection induced by both the temperature gradient and inertial source within square enclosure has been studied. The natural convection effect is attained by temperature gradient between left and right wall (hot and cold respectively). In order to investigate the effect of fan location, three different positions are considered. The study has been carried out by solving numerically momentum and energy equations with the boussinesq approximation. The governing equations have been solved using the finite volume approach, using SIMPLER algorithm on the collocated arrangement. The study has been carried out for the Reynolds number based on the fan diameter in the range of $10 \leq Re \leq 200$, with Rayleigh numbers $10 \leq Ra \leq 10^6$ for three fan position $L_F = 0.2, 0.5$ and 0.8 , while Prandtl number is kept at 0.71 . Results are presented in the form of streamlines, isotherms, and average Nusselt number. The results show that the average Nusselt number increases with increasing in Reynolds number in forced convection regime.

Keywords: forced Convection, mixed Convection, ventilated closed cavity.

1. Introduction:

The convection induced by both the temperature gradient and inertial source within enclosure has been studied in due to several practical applications. The most interests of these flows are encountered in several domains such as cooling of electronic equipment's, solar collectors manufacturing, pollution removal and building sciences. In these situations, the interaction between the buoyancy driven and inertial source flows inside the cavity gives complexes convective regimes, and the overall transport patterns can be very different from those driven by the temperature gradients alone.

Among the first studies on the mixed convection in ventilated cavities, we mention by Baines and Turner [1] in closed space. In the case of opened cavity, Woods et al. [2] shows the existence of two main regimes (displacement and blocked regimes) of ventilation by changing the rate of flow. The same regimes are observed by Allano et al [3], by changing the dimension of the opening zone. Papanicolaou and Jaluria [4] presented numerical results of the influence of the thermal conductivity, Richardson and Reynolds numbers on the average Nusselt number induced by mixed convection within enclosure. Overall, they found that the heat transfer increased with increasing this controlling parameters. By adding a heat sources, in the ventilated rectangular cavity, the same authors (Papanicolaou and Jaluria [5]) showed that the location of the sources strongly influences the flows structures, and a oscillatory behaviour was obtained for $Gr/Re^2 = 50$. The influence of this parameter (Gr/Re^2) on the heat transfer is also demonstrated by Hsu and Wang [6] in the case of mixed convection within cavity with two ventilation ports. Raji et al. [7] studied the mixed convection heat transfer in a ventilated cavity. The numerical results showed the presence of a maximum interaction between the effects of the forced and natural convection, with the existence of different flow regimes, delineated in the $Ra-Re$ plane. Bhoite et al. [8], deals with the problem of mixed convection in shallow enclosure with series of heat generating components; they showed that higher Reynolds numbers tend to create a recirculation region of increasing strength at the core region and that the effect of buoyancy becomes insignificant beyond $Re = 600$. Using the LBM method, Mehrizi et al. [9] investigate the effect of suspension of nanoparticles on mixed convection in square cavity with inlet and outlet ports and hot isothermal obstacle; the authors showed that the heat transfer rate is enhanced, except for Richardson numbers greater or equal to 10. Belgen and Muftuoglu [10] studied cooling strategy in square cavity with ventilation ports and discrete heat source; they determined the optimum hote position by maximizing the global conductance at different Rayleigh and Reynolds numbers. They found that the hote position is off centered in all cases, its optimum position is insensitive to the variation of Ra and Re , and it solely depends on the ventilation ports arrangement, and The Nusselt number depended on the variation of the Richardson number. On the basis of the literature review, it appears that several investigations (Calmidi and Mahajan [11], Mamou [12], Bouriche [13,14], Singh and Sharif [15]) analyzed a number of governing parameters in natural or mixed

convection in open cavities, including thermal sources, fluid properties, supplying fluid velocities and dimension or location of ports.

In the case of closed cavities, no work was reported on mixed convection in ventilated enclosure induced by internal inertial sources. Indeed, the existence of a dynamic internal source will create interaction with the thermal forces, induced by differential heating; causing the creation of a mixed flow. Hence, the aim of the present work is numerical analysis of a mixed convection in ventilated cavity (induced by the inertial source) and differentially heated, using the Finites Volumes method. We focus on the influence of various physical and geometrical parameters on the flow structures that can occur in the heat exchange, while demonstrating the existence of critical operating parameters. The main objective of this study is to analyze the effect of the forced flow on the natural convection cells and the flow profile, for various values of Reynolds number and different fan positions, and determine a position, of source ventilation; witch gives the maximum value of Nusselt number Nu for Rayleigh and Reynolds numbers.

2. Physical problem and governing equations:

The configuration under study is showed in Fig.1, and refers to the two-dimensional (2D) flow in a square cavity of $L \times H$ dimensions, and an enclosure aspect ratio $A=L/H=1$. The cavity is heated differentially along the right and left vertical wall (T_h and T_c respectively), where the horizontal walls are insulated (Adiabatic). A volumetric fan, of diameter "D" and thickness "E", is placed in the middle axe of the cavity at three positions ($X=0.2, 0.5$ and 0.8). This fan operates in the vertical direction in order to ensure the cooling of the hot wall; his wheel turns at constant angular velocity ω . As a result, a pressure gradient " ΔP " is created and modeled in our work, as a momentum generation in the Navier-Stokes equations. The axial and radial aspects ratio are considered constants ($B=C=1/20$). We will investigate the influence of Rayleigh and Reynolds numbers of $[1, 10+6]$ and $[10, 5 \times 10+2(\text{or } 200)]$ respectively, Prandt number of 0.71 .

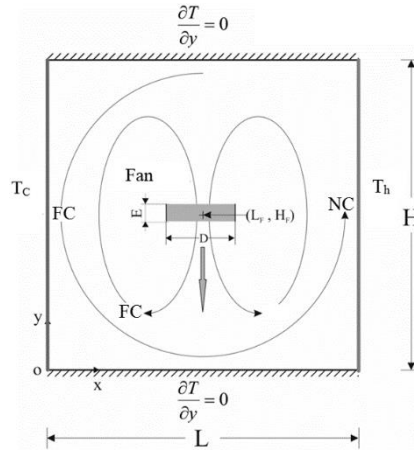


Fig. 1: Physical model

The flow is considered laminar, incompressible and the Boussinesq approximation has been applied. The overpressure ΔP produced by the fan is represented explicitly in momentum equation of (oy) coordinate direction by: $[+\Delta P/E]$, where E is the fan thickness. The dimensional governing equations can be written as:

Continuity equation:

$$\rho \left(\frac{\partial u}{\partial x} + \frac{\partial v}{\partial y} \right) = 0 \quad (1)$$

Momentum equation:

$$\text{ox} : \rho \left(u \frac{\partial u}{\partial x} + v \frac{\partial u}{\partial y} \right) = - \frac{\partial P}{\partial x} + \mu \left(\frac{\partial^2 u}{\partial x^2} + \frac{\partial^2 u}{\partial y^2} \right) \quad (2)$$

$$\text{oy} : \rho \left(u \frac{\partial v}{\partial x} + v \frac{\partial v}{\partial y} \right) = - \frac{\partial P}{\partial y} + \mu \left(\frac{\partial^2 v}{\partial x^2} + \frac{\partial^2 v}{\partial y^2} \right) - \rho \cdot g - \frac{\Delta P}{E} \quad (3)$$

Energy balance equation:

$$u \frac{\partial T}{\partial x} + v \frac{\partial T}{\partial y} = \alpha \left(\frac{\partial^2 T}{\partial x^2} + \frac{\partial^2 T}{\partial y^2} \right) \quad (4)$$

The imposed boundary conditions, in terms of temperature and velocity, are similar to those of the natural convection flow in a rectangular cavity:

$$T(0,y) = T_c, T(L,y) = T_h; \left. \frac{\partial T}{\partial x} \right|_{y=0,L} = 0 \quad (5)$$

$$v(0,y) = v(H,y) = v(x,0) = v(x,H) = 0 \quad (6)$$

Referring to Fig. 1, the dimensionless variables are:

$$x^* = \frac{x}{L}, y^* = \frac{y}{L}, u^* = \frac{u}{\alpha/H}, v^* = \frac{v}{\alpha/H}, p^* = \frac{p}{\rho(\alpha/H)^2}; T^* = \frac{(T - T_c)}{T_h - T_c} \quad (7)$$

The dimensionless governing equations will be written as:

$$\left(\frac{\partial u^*}{\partial x^*} + \frac{\partial v^*}{\partial y^*} \right) = 0 \quad (8)$$

$$\frac{\partial u^*}{\partial t^*} + \left[u \frac{\partial u^*}{\partial x^*} + v \frac{\partial u^*}{\partial y^*} \right] = - \frac{\partial p^*}{\partial x^*} + \text{Pr} \left(\frac{\partial^2 u^*}{\partial x^{*2}} + \frac{\partial^2 u^*}{\partial y^{*2}} \right) \quad (9)$$

$$\frac{\partial v^*}{\partial t^*} + \left[u \frac{\partial v^*}{\partial x^*} + v \frac{\partial v^*}{\partial y^*} \right] = - \frac{\partial p^*}{\partial y^*} + \text{Pr} \left(\frac{\partial^2 v^*}{\partial x^{*2}} + \frac{\partial^2 v^*}{\partial y^{*2}} \right) + \text{Ra} \cdot \text{Pr} \cdot T - \frac{\text{Rt}}{B} \left(\frac{\text{Re}}{C} \cdot \text{Pr} \right)^2 \quad (10)$$

$$u^* \frac{\partial T^*}{\partial x^*} + v^* \frac{\partial T^*}{\partial y^*} = \left(\frac{\partial^2 T^*}{\partial x^{*2}} + \frac{\partial^2 T^*}{\partial y^{*2}} \right) \quad (11)$$

Where R_t denotes the dimensionless Rateau pressure invariant. It represents the relationship between the pressure difference (ΔP) and the kinetic energy ρV_{fan}^2 produced by the ventilator.

The dimensionless numbers are:

$$\text{Pr} = \frac{\nu}{\alpha}; \text{Re} = \frac{V_{\text{fan}} \cdot H}{\nu}; \text{Ra} = \frac{g\beta\Delta TH^3}{\nu\alpha}; \text{Rt} = \frac{\Delta P}{\rho V_{\text{fan}}^2}; V_{\text{fan}} = \omega \cdot \frac{D}{2} \quad (12)$$

$$A = \frac{L}{H}; B = \frac{E}{H}; C = \frac{D}{H} \quad (13)$$

The average Nusselt number at heated walls was calculated as follows:

$$\text{Nu}_H = \frac{1}{H} \int_0^H \text{Nu}_x dy \text{ with } \text{Nu}_x = \int \left. \frac{dT}{dx} \right|_{x=L} \quad (14)$$

3. Numerical method:

All of the governing equations were transformed into sets of algebraic equation based on the finite volume method. The staggered grid system was used. In order to handle convective and diffusion terms, the power law scheme was employed. The SIMPLER algorithm was used to couple the velocity, pressure and temperature fields. In order to get the convergence for all problems, the smaller under-relaxation factors were employed, especially for momentum equations in the cases of higher values of Reynolds number ($\text{Re}=200$). The under-relaxation factors taken are 0.1 for momentum equations and 0.8 for pressure and temperature. The convergence criterion in each case was $(\Phi^{i+1} - \Phi^i)/\Phi^i \leq 10^{-6}$, where Φ can stand for any of the dependent variables (v, u, p, T) and i denotes the iteration number.

In this study uniform grid spacing was employed. In order to determine the proper grid numbers due to accuracy, a grid independence test was conducted for a particular case. Four different grid sizes were tested in the case where $\text{Ra} = 10^6$ and $\text{Re} = 0$. Nusselt number Nu is used as the sensitivity measure of the accuracy of the solution; the results are presented in table 1

Table-1: Sensitivity of the results to the number of nodes.				
	80x80	100x100	120x120	140x140
Re=0	8.898	8.854	8.836	8.824
Erreur %	0.48	0.21	0.12	-

Comparison of the Nusselt number values in the four different cases suggest that two grids size gives nearly the same results (deviation less than 0.12 %). Considering the accuracy, the 120x120 grid size was employed for all calculation.

To make sure that the developed code is performing, a validation test was conducted. Calculations for an air filled square cavity without ventilator for $Ra = 10^3$ to 10^6 were carried out, and the results are shown in table 2. Data from the table shows that the results of the code are very close with those found in previous publications. The maximum difference is 1.26%, and probably caused by the different grids sizes, uniformity of mesh and the computational process.

Table-2: Comparison between results of this work and previous works.				
Reference	Average Nusselt Number			
	$Ra=10^3$	$Ra=10^4$	$Ra=10^5$	$Ra=10^6$
Pericleous and al.[16]	1,128	2.245	4,470	8,898
Ambarita and al. [17]	-	2.228	4.514	8.804
Present work	1,114	2,235	4,506	8,835

1. Results and discussion :

1.1. Stream function and isotherms

Fig.2 shows the flow structures (stream lines functions) and isotherms according to Rayleigh and Reynolds numbers for the fan position $L_F = 0.8$. We notice the presence of a symmetric bi-cells structure for low values of the Rayleigh and Reynolds numbers, characterized by two dominant forced convection cells which occupy the entire cavity (*i.e.* $Re=10$ & 50). Gradually, as the forced convection is enhanced by increasing the Reynolds number (*i.e.* $Re=100$), two Secondary cells appear in the upper corners. When the air jet becomes more intense ($Re=2 \times 10^2$), two small cells are developed by decreasing the size of the two principal cells.

When the Rayleigh number increases, the state of the flow structures remains dependent on the Reynolds number value. For low Reynolds number (low forced convection $Re \leq 10^{+1}$, the bi-cells structure disappears to give rise to the flow structure characterized by a single cell that turns counter-clockwise on account of the thermal gradient direction. In this situation, the flow is by natural convection with a thermal boundary layer profile.

With increasing of Reynolds number, this figure shows that multicellular flow begins losing its symmetry progressively as the right cell develops to the detriment of its counter-rotate one. This spatial competition between natural and forced convection continues even for $Ra = 10^{+6}$, where we see the presence of a contra-rotating cell.

The isotherms corresponding to the different control parameters (*i.e.* Re , Ra ; Reynolds and Rayleigh numbers) lie between 0 and 1, minimum and maximum limit of the dimensionless formulation with 0.1 between two successive isotherms. Unlike the case of the pure natural convection, Fig.2 shows the absence of the thermal stratification within the cavity except for low Reynolds number ($Re=10^{+1}$) where the thermal distortion is reduced. We also note that the temperature distribution is in conformity with the fluid flow revealed by the flow structures (streamlines). This fluid flow tends to twist the isotherms and transport them depending on the direction of the fluid movement. When the natural convection is dominant (*i.e.* $Ra \geq 10^{+6}$), the isotherms are similar to those of natural convection type and the effect of the ventilation becomes negligible and its influence is limited only in the vicinity of the fan.

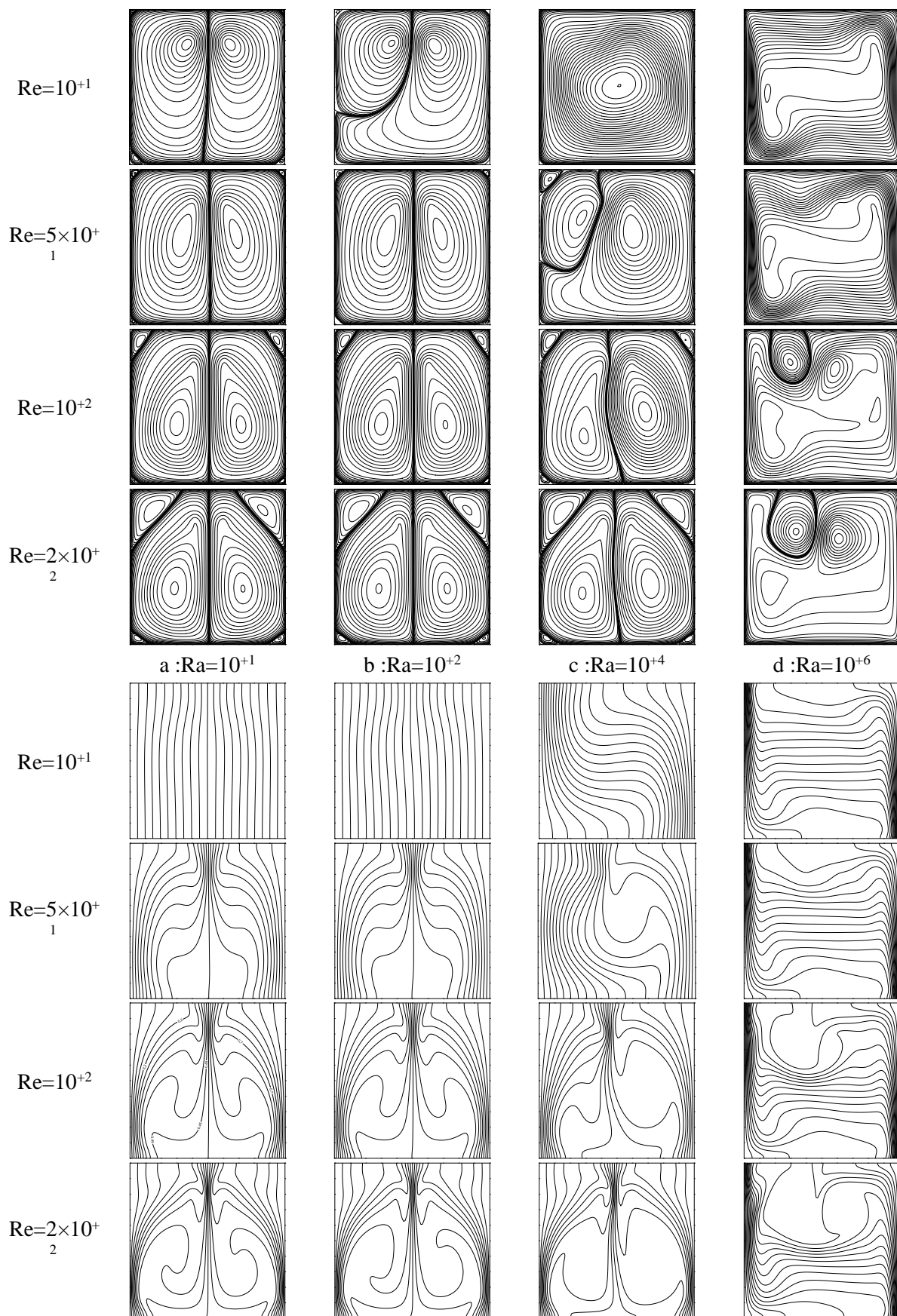


Fig.2 : Stream function and isotherm as function of Reynolds and Rayleigh numbers for $L_F=0.5$ et $H_F=0.8$

To analyze the effect of the horizontal position on the flow structures and the isotherms, two horizontal fan positions were selected $L_F=0.2$ and 0.8 with the vertical position $H_F = 0.8$, and are shown in Fig.3 for different Rayleigh and Reynolds numbers.

For low Rayleigh number values (i.e. $Re \leq 10^4$), we see that the flow structure is composed of a single forced convection cell that occupies the entire field, so that low intensity cells are trapped at the four corners of the cavity. For $L_F=0.2$ the motor cell rotates in the anti-clockwise direction (the same as the buoyancy forces), whereas for $L_F=0.8$ the cell is counter rotate.

When the Rayleigh number increases, the state of the flow is dependent on the Reynolds number and the horizontal position L_F . For the low values of Re (i.e. $Re \leq 10^2$), the motor cell disappears completely to give rise to a flow characterized by a single natural convection cell. In this situation, the flow is of boundary layer type, except for the case ($Re=200$ and $L_F=0.2$) where the motor cell dominates the flow and does not bifurcate. This cell is a combination of the ventilation jet and the buoyancy forces. In this situation, the two forces are cooperating.

For $L_F=0.8$ the rotation direction of cell ventilation is opposite to that imposed by buoyancy forces. As a result, the motor cell is bifurcated and its intensity decreases with the increase of Rayleigh number. For $Ra=10^6$, the effect of ventilation is summarized in the presence of a recirculation cell near the ventilator.

The evolution of isotherms corresponding to the different control parameters (i.e. Reynolds and Rayleigh numbers, as well as the position L_F) show that, contrary to the case of L_F pure natural convection, the absence of thermal stratification within the cavity, which is replaced by strong distortions. It is also noted that the distribution of the temperature is in accordance with the fluid circulation revealed by the stream function. This circulation tends to twist the isotherms and transport them as the direction of the fluid circulation. When the buoyancy forces are higher (i.e. $Ra=10^6$), the isotherms are similar to those of natural convection type, and the ventilation effect becomes negligible and is limited to the vicinity of the ventilator for $L_F=0.8$. Whereas for $L_F=0.2$ and $Re=200$, we notice the absence of thermal stratification and the isotherms are more distorted. In this case, the two forces (dynamic and thermal) are cooperating and the isotherms are tighter near vertical walls, Which makes the greatest transfer rate.

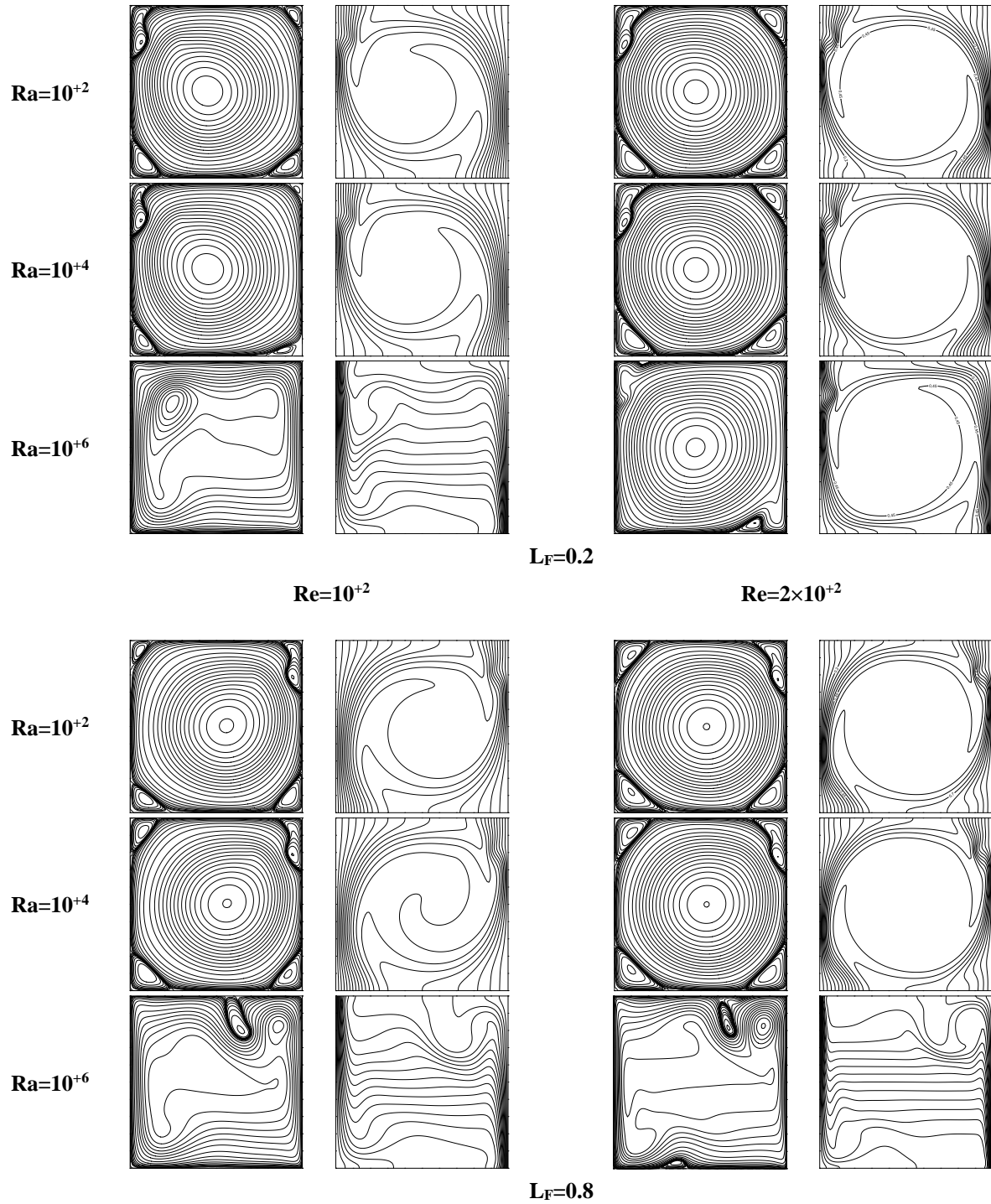


Fig.3 : Stream function and isotherm as function of Reynolds and Rayleigh numbers for $L_F=0.5$ et $H_F=0.8$

1.2. Heat transfer

For low values of Re number, the heat transfer evolution (Nusselt number) is independent of the Re number, characterized by a horizontal line, and this despite the influence of this latter on the flow structure, but not on the isotherms. It should also be mentioned that in this situation ($Re = 10 + 1$), the fan position change has no influence on the heat transfer and its effect is barely perceptible, whatever the Rayleigh value is. It should be mentioned that in all cases, beyond a certain value of Rayleigh number, the influence of the fan position on the heat transfer is negligible and the evolution of the Nusselt number is similar of that of natural convection. In this situation (high values of Ra), the flow tends towards a boundary layer structure and the importance of the forced convection effects tend to disappear.

The effect of the horizontal position L_F on the Nusselt number is illustrated on the Fig.4 as a function of the Rayleigh and Reynolds numbers. Three positions were chosen $L_F=0.2, 0.5$ and 0.8 with $H_F=0.2$. In general, the position $L_F=0.2$ gives slightly higher values for $Re=10$. This advantage is due to the fact that the thermal and dynamic forces are cooperating. At $Ra=10^{+4}$ the flow tends towards a boundary layer structure and the importance of the forced convection effects disappear.

When Re number increases, the heat transfer intensifies and the forced convection is dominant, so the Nusselt number value is always higher for the eccentric positions (i.e. $L_F=0.2$ and 0.8).

For $Re=100$ and 200 the forced convection regime is dominant until a critical Rayleigh value " Rac " which depends essentially on the couple of parameters Re and L_F . When Ra number increases again (i.e. $Ra > Rac$), the Nusselt number curve is uniformly increasing for $H_F=0.2$, whereas it is disturbed for the positions $L_F=0.5$ and 0.8 under the effect of the bifurcation of the flow cells (Fig.4). This passage is directly related to the rotation direction of the ventilation cells (with or against that imposed by the temperature gradient).

In the forced convection mode, the best heat transfers are obtained for a maximum Reynolds number $Re=200$, especially with the eccentric positions of the ventilator ($L_F=0.2$ & 0.8). Thus for $L_F=0.5$ and $Re=200$ the heat transfer rate is almost equal to that found with $L_F=0.2$ and 0.8 , but with a Reynolds number reduced by half (i.e. $Re=100$), i.e. a 50% saving on ventilation energy.

The Nusselt number curves for these last positions are superimposed for $Re=10^{+2}$ and 200 ($Nu = 4.11$ and 6.04 respectively) and the heat transfer is improved by 27% and 31.45% ($L_F = 0.5$) for the same values of Re . This is the advantage of the unicellular profile of the flow under forced convection conditions.

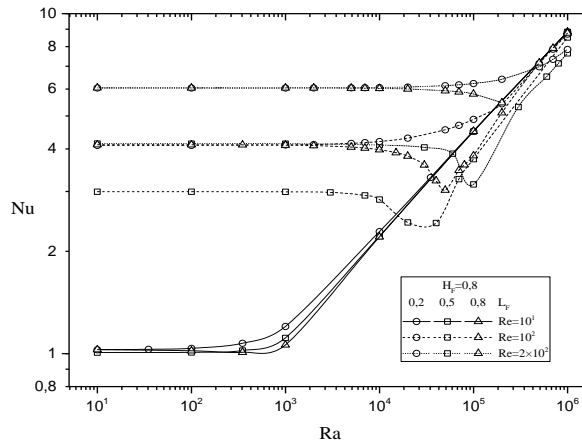


Fig.4 Heat transfer rate as function of Rayleigh number for different values of Reynolds number and fan position L_F .

Conclusion:

The study undertaken and presented in this work, focus on the numerical investigation of the laminar mixed convection in a newtonian fluid flowing in a closed square cavity. In addition to natural convection induced by the temperature gradient between the two active walls, an axial fan is introduced into the cavity and modeled as a generator of momentum.

For the case of low values of the Reynolds number, the flow is similar to that encountered in the case of a differentially heated cavity where a boundary layer develops at the hot wall causing the fluid upward. The results show, according to the values of Re and Ra , two types of flows in space competition; the movement of the natural convection and the forced convection for which flow is multicellular whose number of cells depends on the Reynolds value and the fan position L_F .

The heat transfer analysis shows that it intensifies with increasing Rayleigh number. The average Nusselt number is sensitive to the value of the Reynolds number and position of the fan (the distance fan/hot wall), but only for low Rayleigh number and this dependence disappears when thermal pulling increases and therefore a high Ra .

For the forced convection mode ($10 < Ra < 10^{+4}$), the heat transfer takes its optimal values ($Nu=4.95$) for the pair ($Re=200, L_F=0.2$), namely an increases compared to the positions $L_F=0.5$ and $L_F=0.8$ of 38% and 25% respectively for the same value of Reynolds. In addition, this value is greater than that succeed in the case of heating without ventilation with $Ra=10^{+5}$. This is the benefit of heating with internal ventilation in a closed cavity.

Nomenclature

A	aspect ratio
B	axial aspect ratio
C	radial aspect ratio
D	fan diameter
g	Gravity acceleration
h	Convective exchange coefficient
H	cavity height
k	Thermal conductivity
L	Cavity length
Nu	Nusselt number
P	Pressure
Pr	Prandtl number
Ra	Rayleigh number
Re	Reynolds number
Rt	Rateau number
T	Temperature
U	horizontal velocity
V	vertical velocity
x	Longitudinal coordinate
y	Vertical coordinate
β	Thermal expansion coefficient
ρ	density
ν	cinematic Viscosity
μ	dynamic Viscosity
ε	error

Indices

c	cold
h	hot
F	fan

References

- [1] Baines, W.D., Turner, J.S., Turbulent buoyant convection from a source in a confined region. *Journal of Fluid Mechanics* 37, (1969), 51–80.
- [2] Woods, A.W., Caulfield, C.P., Phillips, J.C., Blocked natural ventilation: the effect of a source mass flux. *Journal of Fluid Mechanics* 495, (2003), 119–133.
- [3] Allano D., Danlos A., Patte-Rouland B., Gonzalez M., Paranthoën P., Ventilation naturelle d'une enceinte soumise à une injection de gaz chauds, Congrès SFT 08, Toulouse, (2008) (ISSN: 1258-164X).
- [4] E. Papanicolaou, Y. Jaluria, Transition to a periodic regime in mixed convection in a square cavity, *J. Fluid Mech.* 239, (1992), 489–509.
- [5] E. Papanicolaou, Y. Jaluria, Computation of turbulent flow in mixed convection in a cavity with a localized heat source, *ASME J. Heat Transfer* 117, (1995), 649–658.
- [6] T.H. Hsu, S.G. Wang, Mixed convection in a rectangular enclosure with discrete heat sources. *Numer. Heat Transf., A Appl.* 38, (2000), 627–652.
- [7] A. Raji, M. Hasnaoui, A. Bahlaoui, Numerical study of natural convection dominated heat transfer in a ventilated cavity: Case of forced flow playing simultaneous assisting and opposing roles, *International Journal of Heat and Fluid Flow* 29, (2008), 1174–1181.
- [8] Bhoite, M.T., Narasimham, G.S.V.L., Krishna Murthy, M.V., Mixed convection in a shallow enclosure with a series of heat generating components. *Int. J. Therm. Sci.* 44, (2005), 121–135.

- [9] Abouei Mehrizi, M. Farhadi, H. Hassanzade Afroozi, K. Sedighi, A.A. Rabienataj Darz, Mixed convection heat transfer in a ventilated cavity with hot obstacle: Effect of nanofluid and outlet port location, *Int. Comm. in Heat and Mass Transfer* 39, (2012), 1000–1008.
- [10] E. Bilgen , A. Muftuoglu, Cooling strategy by mixed convection of a discrete heater at its optimum position in a square cavity with ventilation ports. *Int. Comm. in Heat and Mass Transfer* 35, (2008), 545–550
- [11] Calmidi, V.V., Mahajan, R.L., Mixed convection over a heated horizontal surface in a partial enclosure. *Int. J of Heat Fluid Flow* 19, (1998), 358– 367.
- [12] Mamou, M., Stability analysis of thermosolutal convection in a vertical packed porous enclosure. *Physics of Fluids* 14, (2002), 4302–4314.
- [13] Bourich, M., Amahmid, A., Hasnaoui, M., Double diffusive convection in a porous enclosure submitted to cross gradients of temperature and concentration. *Energy Conversion and Management* 45, (2004), 1655–1670.
- [14] Bourich, M., Hasnaoui, M., Amahmid, A., Double-diffusive natural convection in a porous enclosure partially heated from below and differentially salted. *International Journal of Heat Fluid Flow* 25, (2004), 1034–1046.
- [15] Singh, S., Sharif, M.A.R., Mixed convective cooling of a rectangular cavity with inlet and exit openings on differentially heated side walls. *Numerical Heat Transfer Part A* 44, (2003), 233–253.
- [16] N. C. M. a. K. A. PERICLEOUS, "Laminar and Turbulent Natural Convection in an Enclosed Cavity," *Heat and Mass Transfer*, p. 18, 1983.
- [17] H. Ambarita, K. Kishinami, M. Daimaruya, T. Saitoh, H. Takahashi, and J. Suzuki, "Laminar natural convection heat transfer in an air filled square cavity with two insulated baffles attached to its horizontal walls," *Thermal Science & Engineering*, vol. 14, no. 3, 2006.